AD-A117 900 NAVAL RESEARCH LAB WASHINGTON DC F/G 20/9
MICROWAVE ENERGY COUPLING IN A NITROGEN BREAKDOWN PLASMA.(U)
AUG 82 C L YEE, A W ALI, W M BOLLEN
UNCLASSIFIED NRL-MR-4869 NL

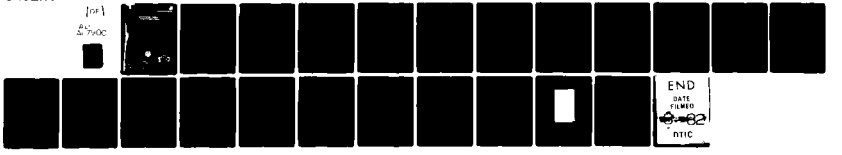

END
DATE FILMED
-82
DTIC

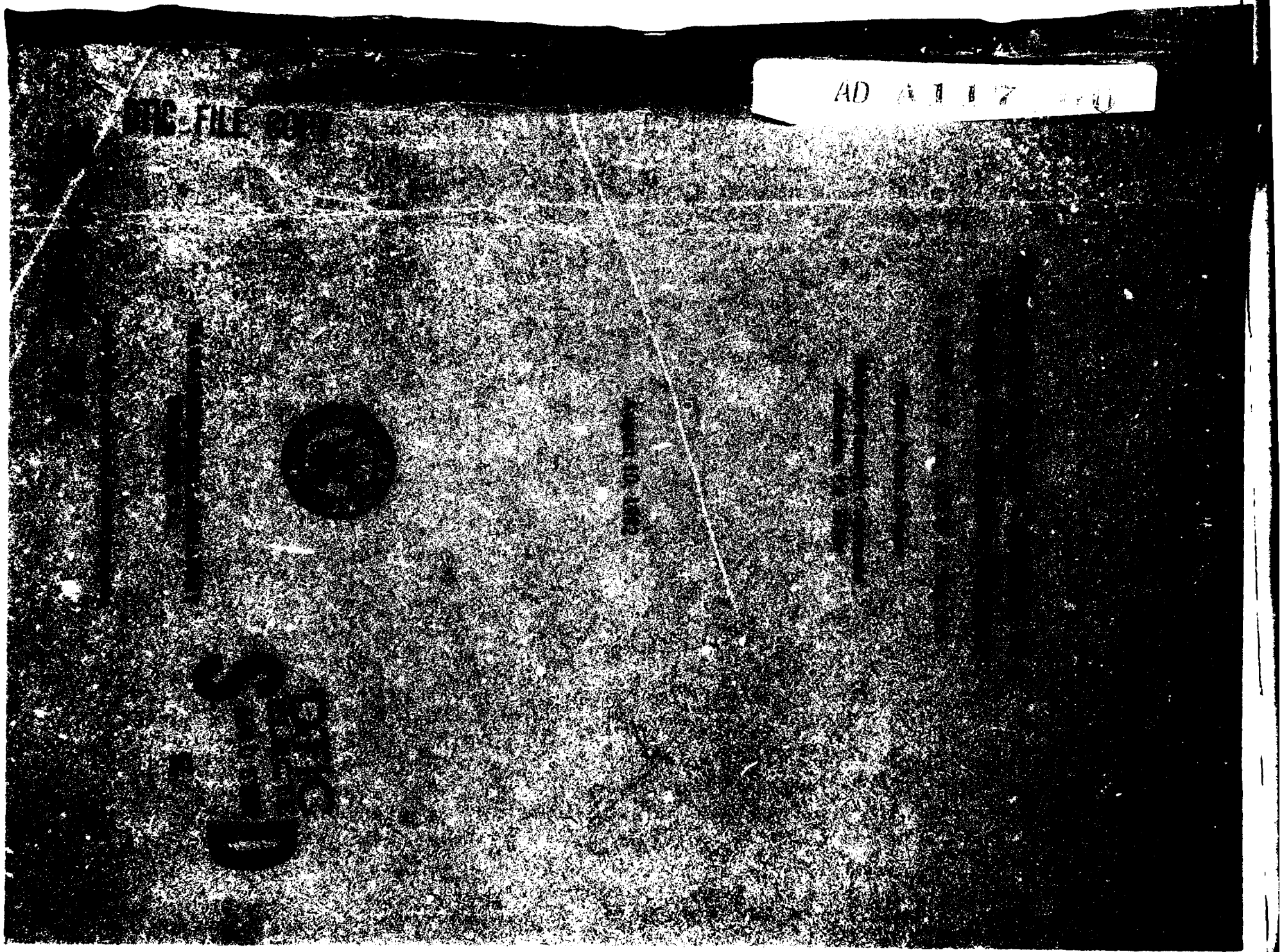

SECURITY CLASSIFICATION OF THIS PAGE (When Data Entered)

REPORT DOCUMENTATION PAGE	READ INSTRUCTIONS BEFORE COMPLETING FORM
1. REPORT NUMBER NRL Memorandum Report 4869	2. GOVT ACCESSION NO. AD-A117900	3. RECIPIENT'S CATALOG NUMBER
4. TITLE (and Subtitle) MICROWAVE ENERGY COUPLING IN A NITROGEN BREAKDOWN PLASMA	5. TYPE OF REPORT & PERIOD COVERED Interim report on a continuing NRL problem. 6. PERFORMING ORG. REPORT NUMBER
7. AUTHOR(s) C.L. Yee*, A.W. Ali, and W.M. Bollen*	8. CONTRACT OR GRANT NUMBER(s)
9. PERFORMING ORGANIZATION NAME AND ADDRESS Naval Research Laboratory Washington, DC 20375	10. PROGRAM ELEMENT, PROJECT, TASK AREA & WORK UNIT NUMBERS NAVSEA, SF-68-344-601; 47-0868-0-2
11. CONTROLLING OFFICE NAME AND ADDRESS Naval Sea Systems Command Washington, DC 20362	12. REPORT DATE August 10, 1982 13. NUMBER OF PAGES 22
14. MONITORING AGENCY NAME & ADDRESS(if different from Controlling Office)	15. SECURITY CLASS. (of this report) UNCLASSIFIED 15a. DECLASSIFICATION/DOWNGRADING SCHEDULE

16. DISTRIBUTION STATEMENT (of this Report)

Approved for public release; distribution unlimited.

17. DISTRIBUTION STATEMENT (of the abstract entered in Block 20, if different from Report)

18. SUPPLEMENTARY NOTES

*Present address: Mission Research Corporation, Alexandria, VA 22304

19. KEY WORDS (Continue on reverse side if necessary and identify by block number)

Microwave
Nitrogen plasma
Energy coupling

20. ABSTRACT (Continue on reverse side if necessary and identify by block number)

Computer simulations of microwave coupling to a nitrogen breakdown plasma have been performed at 25 Torr. Non-hydrodynamic ionization fronts are observed to propagate toward the radiation source under a variety of circumstances. Free nitrogen breakdown simulations in a spherical system show the propagation velocity of the breakdown wave can be as high as 5×10^6 cm/sec. An elementary theory is used for estimating the speed of the breakdown wave in one dimension. The results are in reasonable agreement with breakdown experiments.

DD FORM 1 JAN 73 1473 EDITION OF 1 NOV 65 IS OBSOLETE
S/N 0102-014-6601

SECURITY CLASSIFICATION OF THIS PAGE (When Data Entered)

CONTENTS

MICROWAVE ENERGY COUPLING IN A NITROGEN BREAKDOWN PLASMA

1.0 Introduction

The pulsed breakdown in air and other gaseous elements has been studied extensively[1] with emphasis on the threshold power for breakdown and its dependence on the gas pressure and radiation wavelength. The hydrodynamic effects were first considered by Lin and Theofilos.[2] Their calculation of the gas heating showed that both high field intensity above the breakdown intensity and increasing molecular density discouraged energy deposition in air. Though the preliminary experimental results confirmed the general features of the simple theory, the observed pressure waves were stronger than predicted. Scharfman[3] et al., have observed that a breakdown plasma prevents the transmission of microwave energy to points beyond the plasma. Experiments[4] recently performed at the Naval Research Laboratory (NRL) showed that the microwaves are rapidly decoupled from a target or plasma surface. This rapid decoupling of the microwaves would limit the amount of energy that can be deposited into the gas. Computer simulations of the NRL experiments have been performed at a pressure of 25 Torr in nitrogen. Throughout this work, we have used the MINI code developed at NRL to help in understanding the basic interaction processes in the experiments.

2.0 The Microwave Nitrogen Interaction Code (MINI)

The MIicrowave Nitrogen Interaction code (MINI) used in our studies is an one-dimensional multi-species, multi-temperature, hydrodynamic, nitrogen chemistry and wave optics code. The species followed dynamically were N_2, $N_2^+(X)$, $N_2^+(B)$, N_4^+, N, $N(^2D)$, $N_2(A^3\Sigma)$, $N_2(B^3\pi)$, $N_2(C^3\pi)$, and the electron density (n_e). The model calculates the electron (T_e), vibrational (T_v) and gas (T_g) temperatures, and is space and time dependent with microwave absorption and reflection considered in the wave optics mode. The detail of the chemistry and the wave optics aspect of the code are described elsewhere[5] and will not be repeated here. The electrons are described hydrodynamically by the equations

Manuscript submitted May 14, 1982.

$$\partial_t(n_e) + \nabla\cdot(n_e\vec{u}_e) = C_e$$

$$\vec{u}_e = \vec{u}_m - \mu_e\vec{E} - D_e\vec{\nabla}(\ln n_e) - D_e\vec{\nabla}(\ln T_e)$$

$$\partial_t(\varepsilon_e) + \vec{\nabla}\cdot\{\varepsilon_e\vec{u}_e + p_e\vec{u}_e + \vec{Q}_e\} = \vec{R}_e\cdot\vec{u}_e + \vec{J}_e\cdot\vec{E} + E_e$$

$$\varepsilon_e = \frac{3}{2} n_e T_e + \frac{1}{2} m_e n_e u_e^2$$

where $p_e = n_e T_e$ is the electron pressure, $\vec{J}_e = -en_e\vec{u}_e$ is the electron current density, $\vec{R}_e = -m_e n_e \nu_c(\vec{u}_e - \vec{u}_m)$ is the electron momentum transfer rate, $\mu_e = e/m_e\nu_c$ is the electron mobility, and $D_e = T_e/m_e\nu_c$ is the electron diffusion coefficient. The electron momentum transfer frequency is ν_c, and m_e is the mass of the electron. The electron energy flux is $\vec{Q}_e = -\kappa_e\vec{\nabla}T_e$ where the electron thermal conductivity is $\kappa_e = \beta n_e T_e/m_e\nu_c$ and β is a constant. The terms on the right hand side of the energy equation represent energy lost due to heat flow, work due to momentum transfer, joule heating and heating due to elastic, inelastic, and chemical processes. The term C_e represents sources and sinks terms for the electron due to ionization, recombination, and attachment. The E_e term in the electron energy equation includes energy losses due to vibrational and electronic excitation of molecular nitrogen. The C_e and E_e terms are discussed more fully in Ref. (5). The average velocity of molecular nitrogen, $\vec{u}_m$, is related to the diffusion and mass-average-velocity[6] of the heavy particles by $\vec{u}_m = \vec{v}_m + \vec{u}$. The diffusion velocity is $\vec{v}_m$, and u is the mass-average-velocity of the heavy particles.

The continuity equation for each of the heavy particle species is

$$\partial_t(n_i) + \vec{\nabla}\cdot(n_i\vec{u}_i) = C_i.$$

The momentum equation for the heavy particles is

$$\partial_t(\rho\vec{u}) + \vec{\nabla}\cdot(\rho\vec{u}\vec{u} + \underline{\Pi}) = \rho^+\vec{E} - \vec{R}_e$$

where $\rho = \Sigma_i m_i n_i$, $\rho^+ = \Sigma_i Z_i e n_i$, and $\underline{\Pi} = \underline{\pi} + p_H\underline{I}$ are the mass density, positive charge density, and pressure tensor. The viscous portion of the pressure tensor is $\underline{\pi}$, $p_H = T_g\Sigma_i n_i$ is the heavy particle pressure, and $\underline{I}$ is the unit tensor. The heavy particle energy equation is

$$\partial_t(\varepsilon_H) + \vec{\nabla}\cdot\{\varepsilon_H\vec{u} + \vec{Q}_H + \underline{\Pi}\cdot\vec{u}\} = -\vec{J}_e\cdot\vec{E} + \vec{R}_e\cdot\vec{u}_e + \frac{n}{\tau_v}m\{\varepsilon_v(T_v) - \varepsilon_v(T_g)\} + E_H$$

$$\varepsilon_H = \Sigma_i c_i n_i T_g + \frac{1}{2}\rho u^2$$

where ε_H is the total energy density, c_i is the translation-rotational specific heat, $\varepsilon_v(T_v) = \varepsilon\{\exp(\varepsilon/T_v) - 1\}^{-1}$ is the average vibrational energy per molecule,[7] $\varepsilon \simeq 0.3$ eV is the quantum of vibrational energy for nitrogen, τ_v is the characteristic time for vibrational relaxation,[8] and E_H is the heating terms due to chemical, elastic, and inelastic processes. Again a more detailed discussion of E_H can be found in Ref. (5). The heavy particle energy flux is $\vec{Q}_H = -\kappa_H\vec{\nabla}T_g$, and κ_H is the thermal conductivity of the gas, including translational and rotational contribution.[9] The average and diffusion velocity of species i are related by $\vec{u}_i = \vec{v}_i + \vec{u}$. The diffusion velocity of the ith ion species is $\vec{v}_i$ and $\vec{u}$ is the mass-average-velocity of the heavy particles

$$\vec{u} = \frac{1}{\rho}\Sigma_i m_i n_i\vec{u}_i \simeq \vec{u}_m.$$

The vibrational energy equation may be written approximately as

$$\partial_t\{n_m\varepsilon_v(T_v)\} + \vec{\nabla}\cdot\{n_m\varepsilon_v(T_v)\vec{u}_m + \vec{Q}_v\} = -\frac{n_m}{\tau_v}\{\varepsilon_v(T_v) - \varepsilon_v(T_g)\} + E_v$$

where $\vec{Q_v} = -\kappa_v\vec{\nabla}T_v$ is the vibrational energy flux and κ_v is the vibrational conductivity. The vibrational temperature can be calculated assuming that the nitrogen molecule is a harmonic oscillator and that the vibrational levels have a Boltzman distribution. Hence, the vibrational energy source term E_v is

$$E_v = \varepsilon n_m n_e\{1 - \exp(-\varepsilon/T_v)\}\sum_{v=1}^{8} vX_v\{1 - \exp\{\varepsilon v(T_v - T_e)/T_vT_e\}\}$$

where X_v is the excitation rate coefficient[10] for the vth vibrational level obtained from the experimentally measured cross-sections.[11] The vibrational energy spacing is $\varepsilon \simeq 0.3$ eV for nitrogen.

The equations solved in MINI are:

$$\partial_t(n_e) + \partial_x(n_eu_e) = C_e \tag{1}$$

$$u_e = u_m - \mu_eE - D_e\partial_x(\ln n_e) - D_e\partial_x(\ln T_e) \tag{2}$$

$$\partial_t(\varepsilon_e) + \partial_x\{\varepsilon_eu_e + p_eu_e + Q_e\} = R_eu_e + J_eE + E_e \tag{3}$$

$$\varepsilon_e = \frac{3}{2}n_eT_e + \frac{1}{2}m_en_eu_e^2$$

$$\partial_t(n_i) + \partial_x(n_iu_i) = C_i \tag{4}$$

$$\partial_t(\rho u) + \partial_x\{\rho u^2 + p_H - (\frac{4}{3}\mu + \mu_B)\partial_x u\} = \rho^+E - R_e \tag{5}$$

$$\partial_t(\varepsilon_H) + \partial_x\{\varepsilon_Hu + \{p_H - (\frac{4}{3}\mu + \mu_B)\partial_x u\}u + Q_H\} \tag{6}$$

$$= \frac{n_m}{\tau_v}\{\varepsilon_v(T_v) - \varepsilon_v(T_g)\} - J_eE - R_eu_e + E_H$$

$$\partial_t\{n_m\varepsilon_v(T_v)\} + \partial_x\{n_m\varepsilon_v(T_v)u\} = -\frac{n_m}{\tau_v}\{\varepsilon_v(T_v) - \varepsilon_v(T_g)\} + E_v \qquad (7)$$

where the Kinematic and bulk viscosity coefficients are μ and μ_B. The transport coefficients for the viscosity and thermal conductivity are taken from Bird.[12]

The dc portion of the electric field and the diffusion velocities are determined by demanding the total current

$$\vec{J}_T = \vec{J}_e + \sum_i \vec{J}_i = 0 \qquad (8)$$

where $J_i = Z_i e n_i u_i$ is the current density of the ith ion species. In steady state, each of the ion species satisfies an equation

$$\vec{u}_i = \vec{u}_m + \mu_i \vec{E} - D_i \vec{\nabla}(\ln n_i) - D_i \vec{\nabla}(\ln T_g) \qquad (9)$$

where the ion diffusion coefficient and mobility are related to the collision frequency ν_i by $D_i = T_g/m_i\nu_i$ and $\mu_i = Z_i e/m_i\nu_i$. The mass of the ith ion species is m_i. Summing Eq. (9) for all ion species and using Eq. (8) gives an equation for the ambipolar electric field. Once the ambipolar field is found, Eqs. (9) and (2) are used to solve for the flow velocities of the ions and the electron.

The Eulerian difference equations of Eqs. (1) - (7) are solved using the algorithm of Rubin and Burstein.[13] The scheme is simple, second order in accuracy, and is relatively stable while centering the dissipation terms. The hydrodynamic and chemistry portions are calculated separately in a cycle, assuming the flow velocities of the fluid are weak. The hydrodynamics is determined from the updated values of the chemistry. Hence, the hydrodynamics is considered as a small correction to the chemistry.

3.0 Cascade Ionization of Nitrogen by a Microwave Pulse

Microwave gas breakdown begins when a small number of priming electrons acquire sufficient energy from the electric field to ionize the gas. These priming electrons gain energy when the oscillatory energy of the electrons in the electric field is randomized by collisions into thermal energy. Once an electron has an energy in excess of the ionization energy of the gas, the electron can easily ionize the gas, resulting in the generation of two low energy electrons. The electron avalanche can be described by

$$n_e(t) = n_e(0)\exp(t/\tau_B) \tag{10}$$

where $n_e(t)$ is the electron density at time t, and τ_B is the breakdown time. Physically, τ_B is the time required for an electron to gain the energy needed to ionize the gas.[14] Fig. 1 shows the breakdown time, τ_B(sec), and the electron temperature, T_e(eV), for conditions typical of microwave breakdown of N_2. A high radiation field would promote the electron avalanche by increasing the energy imparted to the electron per collision with the molecule. A high molecular density, however, requires higher intensities for the avalance breakdown. At moderate pressures above 25 Torr, the dominant energy loss mechanism for the electrons is the excitation of the electronic and vibrational modes of the gas. The root-mean-square electric field to density ratio, E/n_m (V-cm^2), does not uniquely define the absorbed energy for an ac electric field. The striped region in Fig. 1 is bounded by the constant intensity line (I) and the constant pressure line (P). The rapid variation in τ_B with increasing intensity allows a breakdown threshold, I_B, to be assigned at the onset of breakdown. The ability to couple microwave energy to a breakdown gas depends sensitively on the breakdown time, τ_B, and the electron density.

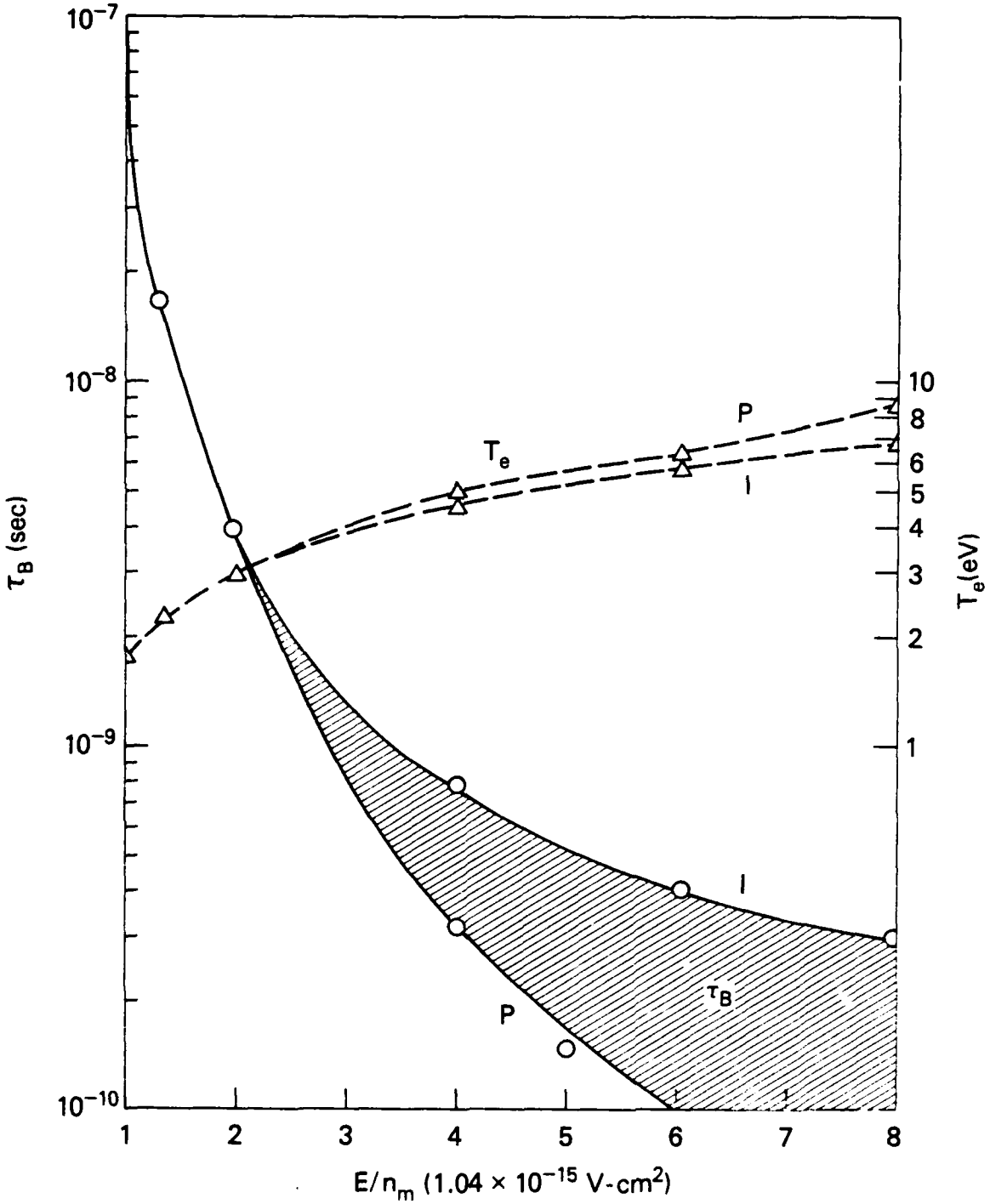

Fig. 1 — The breakdown time and the electron temperature vs the rms electric field to density ratio E/n_m

The efficiency of converting microwave energy to the translational energy of the gas can be enhanced by coupling the microwaves to a preformed plasma. Plasma maintenance of a preformed plasma by microwaves allows the microwave deposition to be localized while maintaining a high electron density. In short pulse breakdown experiments with pulse lengths, $\tau_p < 1$ μsec, a high electron density is a necessary condition for rapid heating of the gas. Plasma maintenance requires the breakdown time $\tau_B > \tau_p$ when $n_e(0) \gg 1$. If the local electric field is not carefully matched to the instantaneous plasma conditions, the gas heating will be self-limited by the formation of a non-hydrodynamic ionization front. Gas breakdown off a reflecting surface without a preformed plasma will not result in a local deposition of the microwave energy. Since the microwave deposition is determined self-consistently with the electron density profile, the resulting plasma density cannot rapidly heat the gas in the short pulse experiments.

3.1 Gas Breakdown Near a Reflecting Surface

A plane wave incident normal to a reflecting surface would require less power for gas breakdown. The constructive interference of the incident and reflected microwave results in the characteristic standing wave pattern for the electric field and a factor of four increase in the field intensity. If the intensity is above the breakdown threshold, breakdown of the gas occurs instantaneously at the peak nodes of the electric field. As the electron density rises, these "pancakes" of electrons begin to attenuate the radiation. Pancakes closest to the reflecting surface rise more rapidly early in the pulse (Fig. 2). As the electron density continues to rise, attenuation of the microwave causes the pancakes closest to the surface to fall in density below that of pancakes far from the surface. Shorter systems with fewer pancakes decouple more rapidly than longer systems. However, the total absorbed energy remains essentially constant, independent of the system size for a fixed pressure and pulse length.[15]

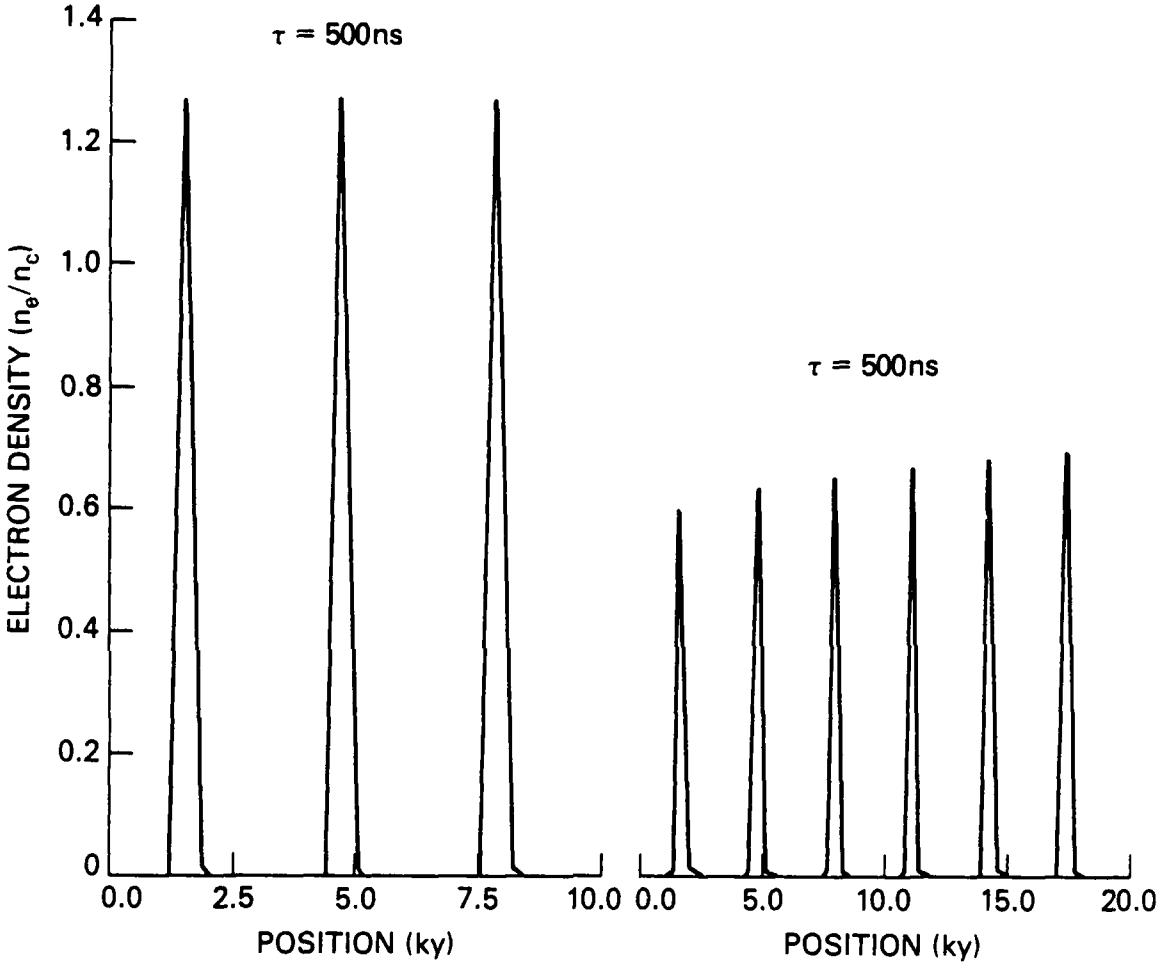

Fig. 2 — Gas breakdown near a reflecting surface showing the electron density pancakes for (a) one-and-a half, and (b) three wavelengths planar system. The critical density is $n_c = 1.5 \times 10^{13}$ cm^{-3} and k = 7.33 cm^{-1}.

The finite length simulations represent the planar region near the surface of a focused microwave system where the distance from the surface is less than the radius of the spotsize. Fig. 2 shows two similar simulations with $I = 6.25\ kW/cm^2$ for an one-and-a-half and three wavelength system without hydrodynamic effects. The plasma absorbs approximately 20% of the total microwave energy with an asymptotic absorption efficiency of 80%. The absorption is regulated by the electron density. Shorter systems have a much higher electron density than larger systems and can more readily heat the gas in the short pulse experiments. The gas is not expected to be heated more than the observed 4% above the ambient temperature in a weakly focused system. The absorbed energy is distributed over a larger number of pancakes with a very low electron density. As will be discussed later, the low electron density of Fig. 2 results in a long heating time for the gas of $\tau_g \simeq 6.5\ \mu sec$ where $\tau_g \equiv T_g(dT_g/dt)^{-1}$. The time required to heat the gas to an appreciable temperature in a weakly focused system would require pulse lengths of $\tau_p \gg 6.5\ \mu sec$. However, even for long pulses, a significant heating of the gas is never realized. Later in the pulse, the pancakes furthest away from the reflecting surface continue to rise in density. Ultimately, a single pancake will have sufficient density to reflect the radiation. This pankcake acts as a secondary reflecting surface and decouples the radiation from the primary metallic surface. Gas breakdown experiments[4] using a reflecting surface show this behavior. Similarly, free nitrogen breakdown simulations without a surface using a focused system also show that the radiation is decoupled from the initial breakdown site.

3.2 Maintenance of a Preformed Plasma by Microwaves

Microwave coupling to a pre-ionized plasma near a metallic surface show some general characteristics. Though the plasma absorbs the microwave energy, the absorption cannot be localized. A traveling ionization front is observed to proceed toward the radiation source. Fig. 3 shows the time history of the ionization front in the strong

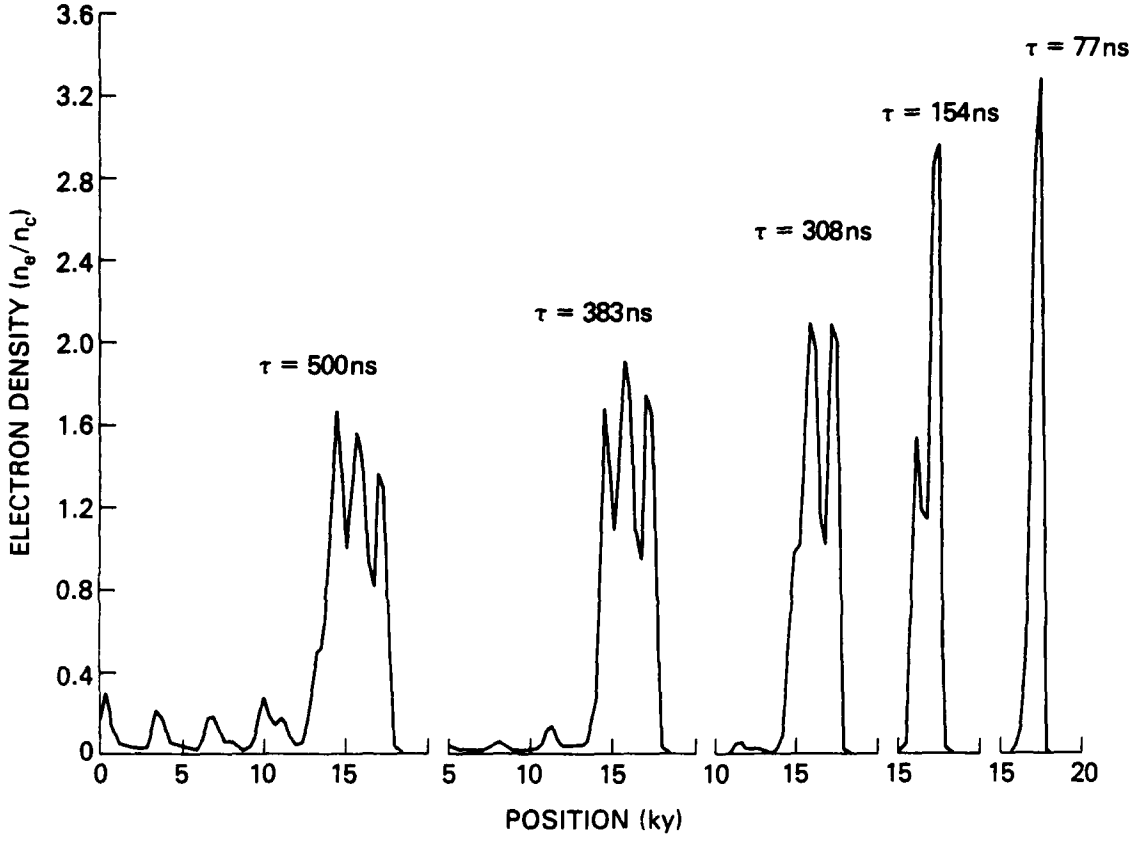

Fig. 3 — Time history of the ionization front in a planar system showing the wave motion toward the radiation source. The microwaves are incident from the left onto a pre-ionized plasma near a reflecting surface on the right boundary. The normalization parameters are the same as in Fig. 2.

mismatch case $I \gg I_B$ and $\tau_p > \tau_c$. The critical time τ_c is the time required for the electron avalanche to reach the critical density $n_c \equiv \omega^2 m_e/4\pi e^2 \simeq 10^{13}/\lambda^2(cm)$ where λ is the wavelength of the incident radiation. In this simulation $I = 12.5$ kW/cm$^2 \gg I_B = 3$ kW/cm^2, $\tau_p = 0.5$ μsec, $\tau_c = 0.16$ μsec, and all hydrodynamic effects are suppresed. The initial electron density (pre-ionized plasma) was initialized with a symmetric profile with a peak density of $0.1n_c$ and FWHM of 0.1λ. In Fig. 3, the peak density is determined by Eq. (10). However, the breakdown time, τ_B, is a complicated function of the incident and reflected microwaves. It is clear that the small reflectivity ($R < 10\%$) is important in determining the propagation speed since as Fig. 3 shows, the separation distance between peaks is $\lambda/4$. The ionization front proceeds toward the source at a characteristic speed $D(t) = \lambda/4\tau_c(t)$. The maximum density is decreasing with time while the total absorption continues to increase with time. The asymptotic absorption efficiency is approximately 95%. The movement of the ionization front limits the time the gas-plasma systems samples the radiation field. The sampling time, τ_s, is determined by $\alpha(cm) = \int_0^{\tau_s} D(t)dt \simeq D(0)\tau_s$ where $D(0) = \lambda/4\tau_c(0) \simeq 1.6 \times 10^6$ cm/sec is the early breakdown speed. Estimating the absorption length as $\alpha(cm) \simeq \lambda/2\pi$ gives a sampling time of $\tau_s \simeq \tau_c$. In the pressure regime $P > 25$ Torr, the gas is primarily heated through the quenching of the electronic states by molecular and atomic nitrogen. The fractional change in the gas temperature is $\varepsilon_g \equiv (\Delta T_g/T_g)_{Max} = \tau_s \Sigma_{\alpha\beta} Q_{\alpha\beta} n_\alpha n_\beta \varepsilon_\alpha / c_v n_m T_g$ where $Q_{\alpha\beta}$ is the quenching rate of the N_2 triplet state n_α by the quenchant n_β. The specific heat of nitrogen is c_v and ε_α is the energy level of the n_α state. As an example, the $N_2(C^3\pi)$ state is quenched by N_2 with a rate coefficient[16] of 1.2×10^{-11} cm^3/sec. The fractional change in the gas temperature, ε_g, is approximately 21% from the ambient temperature.

The region of the maximum gas heating is at the initial breakdown site ($\lambda/4$ from the surface). The electric field is less than

1% of the incident time average electric field at the maximum gas temperature (Fig. 4a). The plasma absorbs approximately 70% of the incident microwave energy and has an electron temperature of less than 2.5 eV (Fig. 4b). Maximum gas heating requires the sampling time and the electron temperature to be as large as possible without decoupling the system. A high electron temperature populates the electronic states which are rapidly quenched to heat the gas. Approximately 4% and 40% of the incident energy goes into heating the gas and exciting the vibrational states. A similar simulation with the peak power reduced to I = 6.25 kW/cm^2 shows no movement of the initial ionization region while increasing the fractional change in the gas temperature to 27%. Further irradiance would increase the gas temperature. However, these results are sensitive to the hydrodynamic response of the plasma. Again, a similar simulation with hydrodynamic effects showed a reduction in the gas and vibrational temperature. The microwave plasma system again decoupled; however, the hydrodynamic motion reduced the energy input into the gas and vibrational energy to 0.1% and 26% respectively. The electron density scale lengths are sharp, $L/\lambda > 10^{-2}$ where $L \equiv n_e(dn_e/dx)^{-1}$. The hydrodynamic motion of the electrons tends to reduce the electron temperature and density in regions of high density. The slow gas flow (< 300 cm/sec) further reduces the electron temperature by convecting the vibrational energy away from regions of high electron density. The small temperature and density changes translate to greater than 10% reduction in the population of the electronic states. Since quenching of the electronic state is the dominant mechanism for rapidly heating the gas, the gas heating is negligibly small. It is clear that the motion of the ionization front will certainly limit the gas heating.

3.3 Gas Breakdown in a Focused Microwave System

Simulations of a focused microwave system were also performed. If the field intensity in a focused system greatly exceeds the breakdown threshold at the focal spot, a breakdown wave propagates toward the source.[17] The motion of the microwave plasma absorbing layer is not a

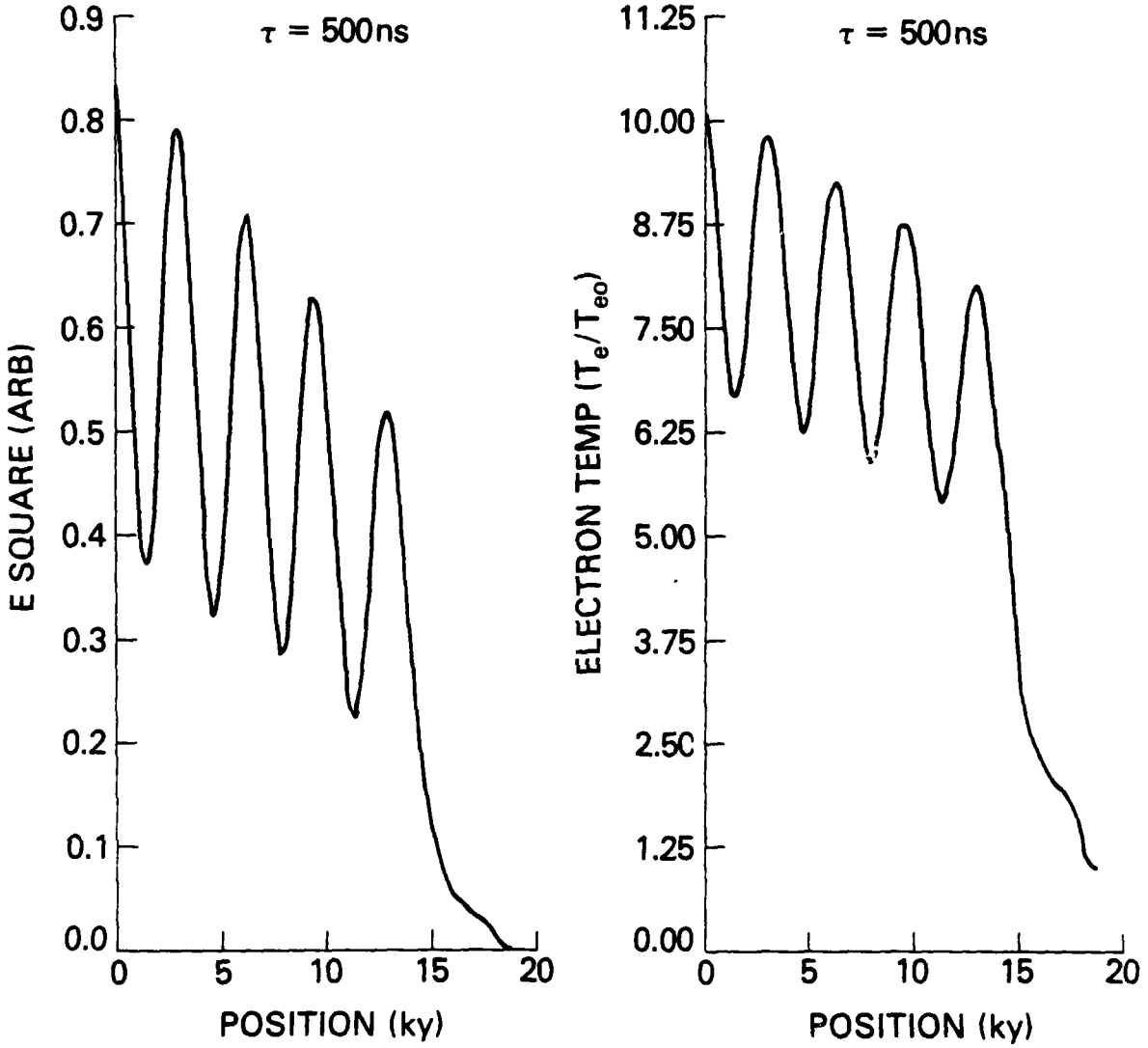

Fig. 4 — (a) The time averaged electric field square and (b) the electron temperature vs position. The normalization parameters are: T_{eO} = 0.25 eV, k = 7.33 cm^{-1}, and the arbitrary units of $<E^2>$ = 1 corresponds to an average intensity of 9.4 kW/cm^2.

simple breakdown wave, since the reflected microwave is important in determining the propagation speed. Fig. 5 shows the time history of the electron density profile during the course of a τ_p = 0.5 μsec pulse in a focused system. The spherical wave equation is solved for the electric field to model the convergence of the field. The peak incident field is I = 10 kW/cm^2 with a system aspect ratio of 2.5. The average power at focus is 31.25 kW/cm^2, and all hydrodynamic effects are suppressed. The very rapid early time speed of the absorbing wave, D ≈ 5 x 10^6 cm/sec, gives a sampling time of $\tau_S \approx 1.7 \times 10^{-8}$ sec. However, the gas continues to be heated after the passage of the field by the de-excitation of the electronic states. The maximum gas and vibrational temperatures are $\varepsilon_g \approx$ 10% and $\varepsilon_v \approx$ 260% respectively. The quarter-wavelength fine structure in the density profile shows the effect of the reflected light. The time average reflection and absorption coefficient are 19% and 68% respectively. A snapshot of the electric field and electron temperature (Fig. 6) shows the lack of field penetration ($\alpha \approx 0.1\lambda$) and the cold plasma temperature, $T_e < 3.3$ eV. The gas and vibrational temperatures again are reduced when hydrodynamic effects are included in the simulations. The gas is expected to be heated, at most, to 10% of the initial value during the course of a 0.5 μsec pulse.

The propagation velocity of the breakdown wave in a focused microwave system can be calculated. Simulations show the absorption is localized at the head of the breakdown wave. The reflection coefficient is relatively constant after the initial breakdown ($t > \tau_C$). The breakdown time, τ_B, is inversely proportional to the light flux, $1/\tau_B \propto (1 + 2Re\zeta + \zeta^2)I$, where the reflection coefficient is ζ^2. The intensity in a conically focused system can be written as

$$I(X,t) \propto \frac{(1 + 2Re\zeta + \zeta^2)}{r^2} \times \phi(t)$$

where $\phi(t)$ is a form function characterizing the pulse. The radius of the radiation channel at a position X on the channel axis is $r = r_0 + X\tan\theta$. The minumum radius of the waist at the focal point is r_0 and θ is the half-angle of the radiation column. Following Raizer,[17] the propagation velocity of the breakdown wave is approximately $D = r_0/\tau_C\tan\theta$. Under the assumptions made, the velocity D would be an upper bound on the propagation velocity of the breakdown wave.

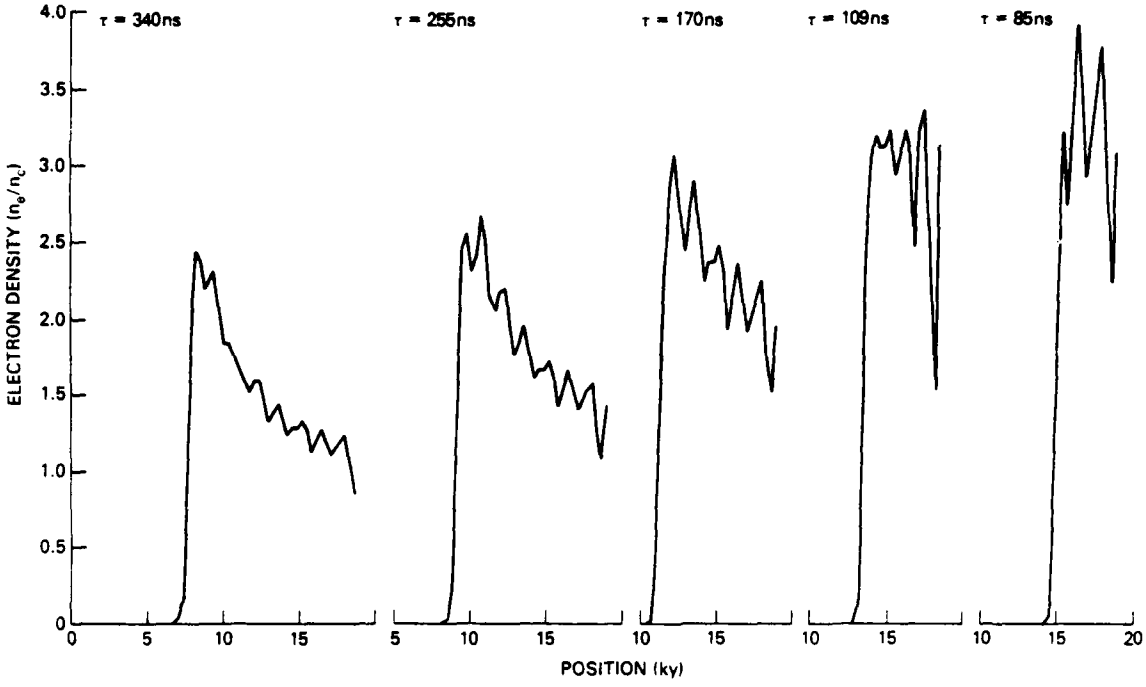

Fig. 5 — Time history of the ionization front in a spherical system. The microwaves are incident from the left boundary with an intensity of 5 kW/cm^2. The focused average power is 31.25 kW/cm^2 at the right side boundary.

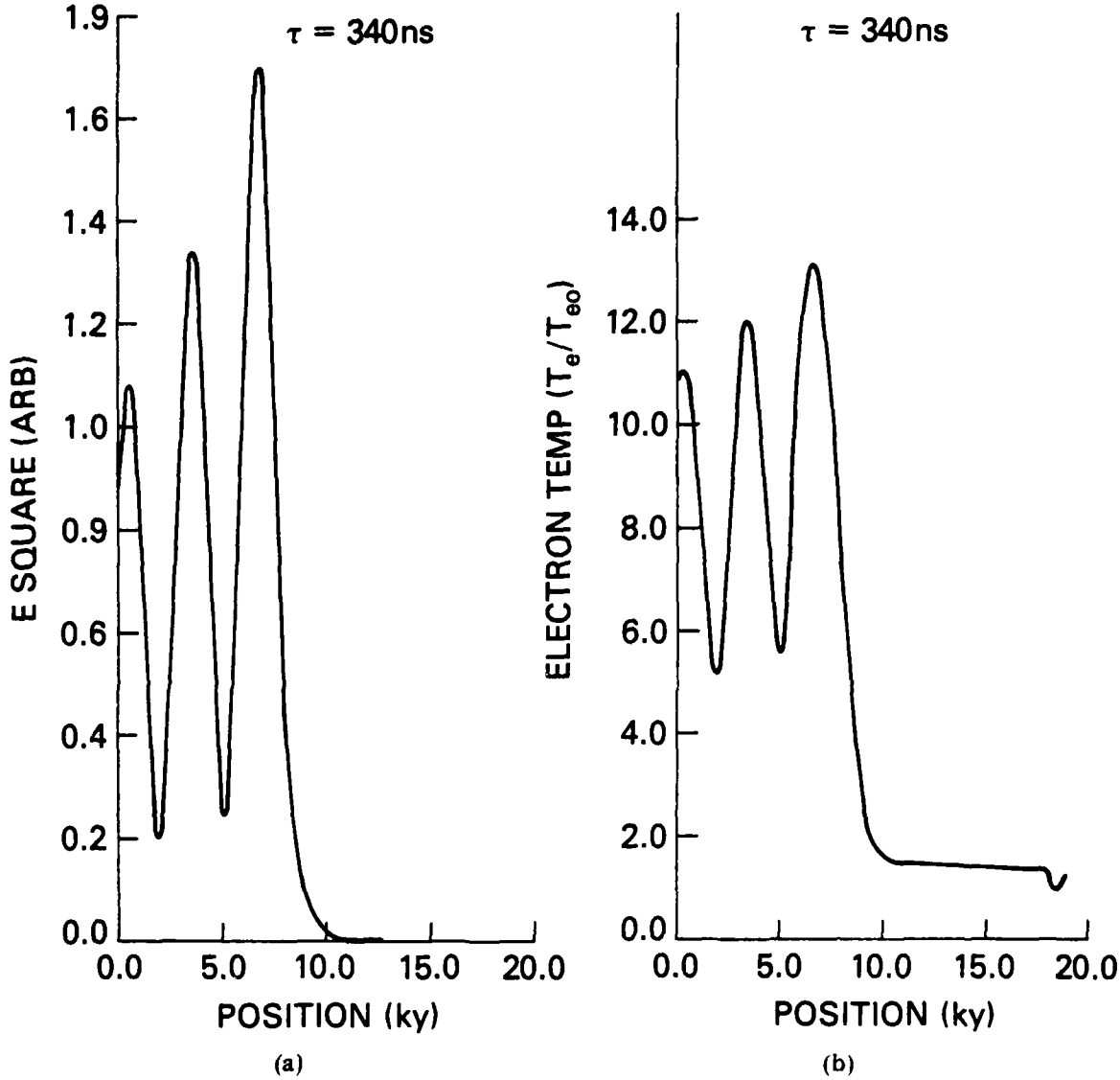

Fig. 6 — (a) The time averaged electric field square and (b) the electron temperature vs position for the simulation of Fig. 5. The normalization parameters are the same as in Fig. 4.

4.0 Simulation of the NRL Experiments

We compare the simulation results with the NRL experiment. The NRL 35 GHz 112 kW focused gyrotron system gives an average power at the focal spot of 33 kW/cm^2. The polarization of the microwave is such that the electric field is perpendicular to the plasma gradient (S polarization). The average aspect ratio of the experiment gives an equivalent simulation aspect ratio of 2.5. The free nitrogen breakdown experiments were performed at 25 Torr with a 100 pps repetition rate at τ_p = 1.5 μsec. The minimum radius of the waist at the focal spot is r_0 = 0.75 cm and the half-angle of the radiation column satisfies $\tan\theta$ = 0.35. Experimentally, framing camera data (Fig. 7) gives a propagation velocity of D ≈ 4.6×10^6 cm/sec. The width of the absorbing wave is approximately 1.2 cm. The measured absolute intensity of the second positive band, N_2 2P (0-0) at 3371 Å is 1.4×10^{21} eV/cm^2-sec. The calculated spatial width of the 3371 Å light emission is 0.8 cm with a peak intensity of 1.8×10^{21} eV/cm^2-sec. As mentioned previously, the calculated speed of the breakdown wave is 5×10^6 cm/sec. Experimentally, the inferred breakdown time is $\tau_B \simeq 2.5 \times 10^{-8}$ sec or $\tau_C \simeq 7.4 \times 10^{-7}$ sec. This is to be compared to the calculated breakdown time early in the pulse, $\tau_B \simeq 4.5 \times 10^{-9}$ sec, and late in the pulse, $\tau_B \simeq 6 \times 10^{-8}$ sec. The simulation results are felt to be in reasonable agreement with the experiment.

5.0 Conclusion

In conclusion, computer simulation of microwave coupling to a weakly ionized nitrogen gas plasma shows excellent absorption of the microwave energy. The electronic states of nitrogen excited by electron impact are rapidly quenched by molecular and atomic nitrogen to heat the gas at pressures above 25 Torr. However, high power irradiance can easily produce a non-hydrodynamic ionization front which can severely limit the heating of the gas. Microwave gas breakdown experiments with pulse lengths less than one microsecond are expected to show only a slight heating of the gas.

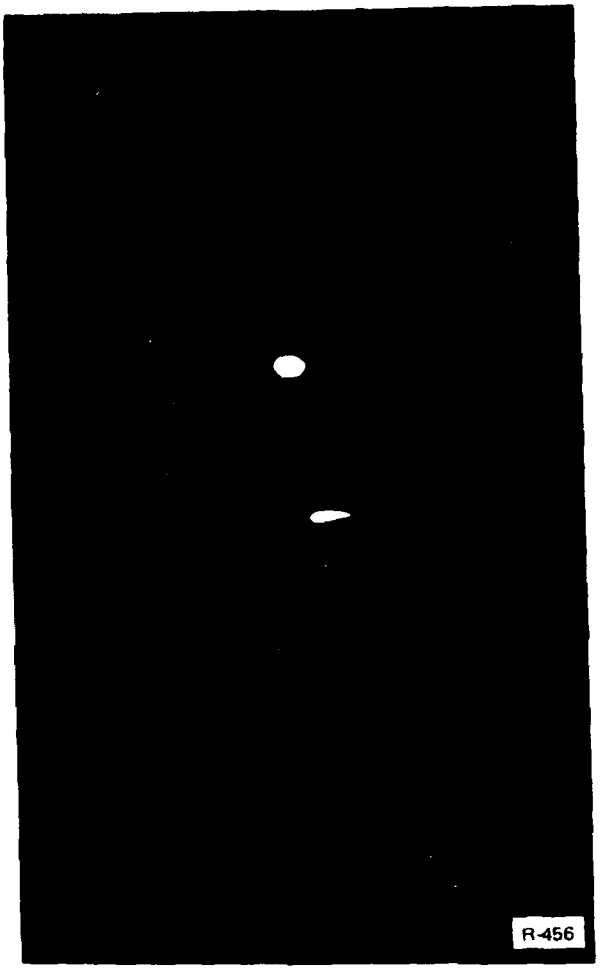

Fig. 7 — Framing camera data showing the motion of the ionization front in a focused free nitrogen breakdown experiment. The top and bottom photographs were respectively taken 0.2- and 0.1- μsec after the first observable breakdown.

REFERENCES

1. A. D. MacDonald, Microwave Breakdown in Gases, John Wiley and Sons, Inc. (New York, 1966).

2. S. C. Lin and G. P. Theofilos, Phys. Fluid 6, 1369 (1963).

3. W. F. Scharfman, et al., IEEE Trans. Antennas and Propagation 12, 709 (1964).

4. W. M. Bollen, et al., "High Power Microwave Energy Coupling to Nitrogen During Breakdown," NRL Memo Report (in press).

5. C. L. Yee and A. W. Ali, "Microwave Energy Deposition, Breakdown and Heating of Nitrogen and Air," NRL Memo Report 4617 (1981).

6. J. O. Hirschfelder, C. F. Curtiss, and R. B. Bird, Molecular Theory of Gases and Liquids, John Wiley and Sons, Inc. (New York, 1964).

7. J. W. Rich, J. Appl, Phys. 42, 2719 (1971).

8. R. Millikan and D. White, J. Chem. Phys. 39, 3209 (1963).

9. Kinetic Processes in Gases and Plasma, edited by A. R. Hochstim (Academic, New York, 1969), Chaps. 2 and 3.

10. A. W. Ali, "The Physics and Chemistry of Two NRL Codes for the Disturbed E and F Regions," NRL Memo Report 7578 (1973).

11. G. J. Schulz, Phys. Rev. 135, A 988 (1964); H. Ehrhardt and R. Willman, Zeits, Phys. 204, 462 (1967); A. G. Engelhardt, et al., Phys. Rev. 135, A 1566 (1964).

12. R. B. Bird, Transport Phenomena, John Wiley and Sons, Inc. (New York, 1960).

13. E. L. Rubin and S. Z. Burstein, J. Computational Phys. 2, 178 (1967).

14. Y. B. Zel'Dovich and Y. P. Raizer, Soviet Physics JETP 20, 772 (1965).

15. Wee Woo and J. S. DeGroot, "Analysis and Computations of Microwave-Atmospheric Interaction," University of California, Davis, Department of Applied Science, Plasma Research Group Report 1981.

16. P. Millet, et al., J. Chem. Phys. 58, 5839 (1973).

17. Y. P. Raizer, Soviet Physics JETP 21, 1009 (1965).

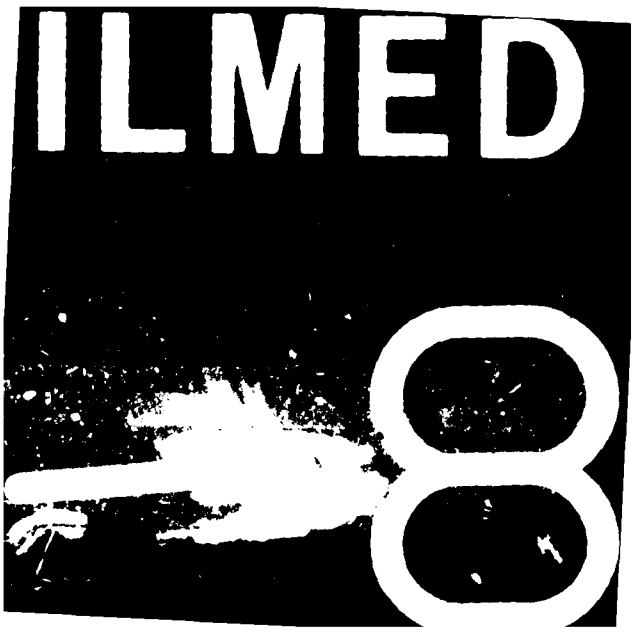
ILMED
8